ORIGINAL ARTICLE

Optimal Parameters of OUPFC and GUPFC Under Renewable Energy Power Variation Using Cuckoo Search Algorithm Variants

K. V. Kumar Kavuturu[1] · **P. V. R. L. Narasimham[2]**

Introduction In this paper, improved variants of cuckoo search algorithm are proposed for optimizing the controlling variables of flexible ac transmission system devices towards voltage stability enhancement and active power loss minimization by considering renewable energy sources intermittency in the network.
Materials and methods Primarily, the optimal location for flexible ac transmission system devices is determined using line stability index and later the control parameters of generalized unified power flow controller and optimal unified power flow controller are optimized at different intermittency levels of renewable energy sources using three cuckoo search algorithm variants. The case studies are performed on standard IEEE 14-, 30-, 57-bus test systems.
Conclusion The superiority of proposed cuckoo search algorithm variants (linearly increased switching parameter, exponentially increased switching parameter and increased switching parameter in a power of three) in solving the multi-objective, non-linear complex optimization problem over time varying acceleration coefficient—particle swarm optimization variants is presented by illustrating various case studies.

Keywords Transmission loss · Line stability index (LSI) · Generalized unified power flow controller (GUPFC) · Optimal unified power flow controller (OUPFC) · Cuckoo search algorithm (CSA) · Renewable energy source intermittency (RESI)

Abbreviations

RES	Renewable energy sources
CES	Conventional energy sources
FACTS	Flexible Ac transmission system
UPFC	Unified power flow controller
OUPFC	Optimal unified power flow controller
PST	Phase shift transformer
GUPFC	Generalized unified power flow controller
CSA	Cuckoo search algorithm
AVDI	Average voltage deviation index
TVAC—PSO	Time varying acceleration coefficients—particle swarm optimization

✉ K. V. Kumar Kavuturu
vasishta.kavuturu@gmail.com

P. V. R. L. Narasimham
drpvrln@gmail.com

[1] Department of Electrical and Electronics Engineering, JNT University, Kakinada, India

[2] Department of Electrical and Electronics Engineering, VR Siddhartha Engineering College, Vijayawada, India

1 Introduction

With the continuing increase in demand and unexpanded transmission system due to limitations, the power systems have been forced to operate closer to the stability limits. To overcome this, integration of renewable energy sources (RES) in every power system is increasing continuously by the adoption of decarbonization policy across the world [1]. Among various types of RES [2], wind and solar photovoltaic based energy sources are the most adopting technologies even at end-user level. As compared to Conventional energy sources (CES), the RES have various advantages like (i) reduced active power losses, (ii) improved voltage profile, (iii) increased overall energy efficiency, (iv) congestion relief across the network elements, (v) potential increase of service quality to the end-customers etc., however the intermittency nature of RES need to be addressed by the researchers.

In recent times, the voltage instability becomes one of the major concerns in power system operation and it has been experienced in many networks across the world. The reports on many power system blackouts reveal the need of transmission system expansion, upgradation and VAr compensation with the advanced technologies [3, 4]. In addition

to the voltage stability, transmission loss is another important operational aspect to concern for economic as well as efficient operation. Real power loss should be minimized for economic reasons and reactive power loss should be minimized to reduce investments in reactive power devices. Both the losses are highly dependent on voltage profile as well as reactive power flows [5, 6]. Thus to minimize losses, it is desirable to have sufficient reactive power reserves by controlling the reactive power flows and keeping better voltage profile across the network.

The flexible ac transmission system (FACTS) devices have been emerged in various networks across the world due to their ability to control as well as to prevent various likelihood uncertainties in real-time operation [7, 8]. A comprehensive literature survey on different types of FACTS devices used in various power system stability studies can be found in [9]. Among the FACTS devices, the 2nd generation FACTS devices like Unified Power Flow Controller (UPFC) [10] and Interline Power Flow Controller (IPFC) [11] have wide range of applications in power system operation and control. UPFC is a versatile device and able to control the power flow parameters of a line (i.e., bus voltage, phase angle and line reactance) individually or in combination. IPFC is able to control power flows in multiple transmission lines at a substation simultaneously or consecutively. The advanced version of UPFC by integrating conventional Phase Shift Transformer (PST) is proposed as Optimal Unified Power Flow Controller (OUPFC) with its operating features and steady-state mathematical modeling [12]. Similarly, improved version of IPFC by including Shunt Compensation is proposed as Generalized Unified Power Flow Controller (GUPFC) in [13].

In specific, each FACTS device is designed for controlling some specific attributes of power system predominately and has own mode of operation, the location should be optimized to get better results. One of the challenging problems after deregulation is congestion management (CM). Basically CM is not a new problem and treated as transmission security management before deregulation era. Many researchers have well addressed the FACTS devices optimal location in literature [14, 15]. The review is recommended the application of FACTS devices is further needed to apply for system security enhancement under contingencies and variations in load and generation pattern. In [16], static var compensator, thyristor controlled series compensator and UPFC devices have been considered for minimizing the multi-objective function formed with real power loss, voltage deviation and generators operating cost using brain strom optimization algorithm. In [17], moth flame optimization (MFO) and JAYA blended MFO (J-MFO) algorithms have been used for optimizing the location and parameters of static var compensator (SVC) and thyristor controlled series capacitor (TCSC) devices towards loss minimization and installation cost of SVC and TCSC.

In [18], power system security enhancement using optimal controls of static synchronous series compensator and standard blackout model has been proposed for minimizing the risk of cascaded tripping to avoid blackout. The problem of optimal location and sizing of SCCC is solved aimed using an improved particle swarm optimization by aiming the minimization of generators' redispatch cost and load shedding costs. In [19], operating cost of generation, real and reactive power losses, voltage deviation and installation cost of multiple TCSC devices are considered for determining the optimal locations and sizes of multiple TCSC devices using adaptive multi objective parallel seeker optimization algorithm. In [20], optimal power flow (OPF) problem is solved considering the TCSC controls in the power system at best locations using based improved comprehensive-learning particle swarm optimization algorithm. In [21], optimal location and parameters of TCSC have been determined using moth swarm algorithm for minimizing the amount of load to be shed and improving the system performance under normal and contingency conditions. In [22], instead of instead of FACTS devices, optimal location and sizing photovoltaic system has proposed for mitigating the congestion effect. All these works have shown the effectiveness of FACTs devices for managing the power system insecurity conditions. Also, it is observed that the problem of location and sizing of multi-type, multiple FACTS devices towards multiple objectives considering various operational constraints of the power system is a complex and non-linear optimization problem. Many researchers have been contributed for solving this problem using various approaches. An updated review on various methods used for optimal location and sizing of different FACTS devices can be found in [23]. As observed in [23], limited works are only focused on particularly OUPFC even though it is improved version of GUPFC as well as most effective than other FACTS devices. Hence, we considered GUPFC and OUPFC and a comparative study are presented.

In a broad manner, the solutions for optimal location of FACTS devices problem can be classified into three categories like direct, strategic and optimization problem based approaches. In direct approaches, the impact on a specific parameter is analyzed directly by integrating FACTS devices at a selected location. Based on the significant impact on a specified parameter, the locations are further ranked to finalize optimal location. The computational effort involved in direct approaches can overcome by using strategic approaches. These approaches are basically based on sensitivity analysis with control variables in load flow study. By analyzing the impact of change in control variable on a specific attribute, the location of FACTS devices is finalized. Similarly, various heuristic approaches which have been widely used for FACTS location and sizing can be found in [24].

As per no-free-lunch theorem [56], there is no such algorithm which can suit for all kind of optimization problems and hence, the researchers are still inspiring to develop new heuristic algorithms. In this work, we have explored the capabilities of improved CSA variants in solved well defined optimization problem in power system with FACTS devices. In recent times, cuckoo search algorithm (CSA) has adopted for various engineering optimization problems and its comprehensive literature survey can be found in [25]. Some of the power system engineering problems solved by CSA are presented here. In [26, 27], SVC parameters have been optimized using CSA for minimizing the active power loss, voltage deviation, and investment cost of SVC. In [28], hybrid cuckoo search algorithm (HCSA) by adopting crossover operation instead of Levy flight operator has been proposed to solve single and multi-objective optimization problems with generation fuel cost, emission, and total power losses as objectives. In [29], the performance of different FACTS devices for automatic generation control with optimized 2 degrees of freedom controllers in a multi-area power system has been presented. The comparative results of various existing heuristic algorithm have shown that CSA with Levy flights superiority in terms of fast convergence characteristics. In [30], optimal tuning of power system stabilizers parameter (PSS) in a multi-machine power system has been proposed using CS algorithm. The performance of CSA-based PSSs has compared with genetic algorithm (GA) based PSSs parameters and system has attained good damping characteristics with CS-based PSSs than GA-based PSSs. The CSA based optimal design of static synchronous compensator has been proposed for loadability enhancement in a multi-machine power system [31]. The results have been compared with GA and proved CSA superiority in terms of fast convergence characteristics. In [32], power system voltage stability has been improved by optimizing the FACTS devices parameters using teaching learning based optimization (TLBO) technique and CSA. In fact, the TLBO has shown better performance than CSA in this work. In [33], Levy-CSA based OPF has been proposed to determine optimal ratings of TCSC rating for enhancing the line voltage stability. In [34], the UPFC parameters have been optimized for real power cost minimization using CSA. Lévy Flight and Random Walk techniques of the CS are used with the collision techniques of chemical reaction optimization CRO for optimizing UPFC location and its parameters for attaining high voltage quality, minimum active and reactive power losses and installation cost [35].

The major contributions and highlights of this paper claimed are as follows:

- Most of the reviewed works have not considered the nature of RES intermittency.

- A multi-objective function using real power loss and voltage deviation index is formulated considering power injection modeling OUPFC and GUPFC devices and RES intermittency.
- A strategic approach for optimal location of FACTS devices is presented based on line ranking using line stability index (LSI) [36]. In order to explore the effectiveness of OUPFC and GUPFC devices on redistribution of power flows clearly, the lines which already incident to tap-changers and generator buses and shunt VAr devices are excluded in the ranking process.
- The objective function is solved using improved variant of CSA [37, 38] considering different RES intermittency.
- The effectiveness of proposed CSA variants in tuning various parameters of system and FACTS devices for different RES intermittency levels towards objective function are compared with TVAC-PSO algorithm [39, 55].
- The simulation results on IEEE 14-, 30- and 57-bus are shown the capability of OUPFC over GUPFC for maintain system operation satisfactorily with minimum losses, improved voltage profile and enhanced voltage stability.
- The effectiveness of CSA with increased switching parameter in a power of three is presented and the comparative study has shown its superiority over other variants as well as TVAC-PSO in terms of reduced objective function and computational time.

The rest of the paper is organized as follows: Sect. 2 is explored the power injection modeling of GUPFC and OUPFC. Also, the strategic approach followed to identify location of FACTS devices is covered. In Sect. 3, formation of proposed multi-objective optimization problem is explained including RES intermittency modeling. In Sect. 4, the improved variants of CSA and its application to solve the proposed optimization problem are explained. In Sect. 5, the effectiveness of proposed CSA variants is explained using simulation results on IEEE 14-, 30- and 57-bus systems are explained for different RES intermittency scenarios.

2 Modeling and Location of FACTS Devices

The latest generation FACTS devices namely GUPFC and OUPFC are implemented in this paper. Mainly there are two types of modeling namely power injection model (PIM) and current injection models (CIM) are employed for FACTS devices. PIM is more stable and easy to analyze when compared with the CIM [40]. CIM can easily be adopted for conventional analysis but there is a difficulty in solving it, as the injected current depends on the terminal voltage of the FACTS device, iterative techniques must be used to solve it [41]. The PIM of FACTS devices are employed widely in literature due to simple form and easy to implement in NR load flow study

without modifying the Jacobian matrix. In this section, the PIM of OUPFC [12, 42] and GUPFC [13, 43, 44] is reviewed.

2.1 GUPFC

The single line diagram of IPFC and GUPFC are given in Fig. 1a and b respectively. Generally, the IPFC consists of multiple series converters coupled with injection transformers and integrated into multiple transmission lines where as GUPFC has an extra shunt converter at common bus in its configuration. In other way, the UPFC configuration with multiple series converters can also be considered as equivalent of GUPFC.

By considering shunt converter at *bus-i* and series converters in the lines *i-j* and *i-k*, then the power injections at all the incident buses are as follows:

The power injections at shunt converter bus *i* are:

$$P_{inj,i} = \sum_n r_{i-n} b_{s,i-n} V_i V_n \sin\left(\theta_{i-n} + \gamma_{se,i-n}\right), \ n = j, k \tag{1}$$

$$Q_{inj,i} = \sum_n r_{i-n} b_{s,i-n} V_i^2 \cos\left(\gamma_{se,i-n}\right) + Q_{sh,i}, \ n = j, k \tag{2}$$

The power injections at series converter bus *j* are:

$$P_{inj,j} = -r_{i-j} b_{s,i-j} V_i V_j \sin\left(\theta_{i-j} + \gamma_{se,i-j}\right) \tag{3}$$

$$Q_{inj,j} = -r_{i-j} b_{s,i-j} V_i V_j \cos\left(\theta_{i-j} + \gamma_{se,i-j}\right) \tag{4}$$

The power injections at series converter bus *k* are:

$$P_{inj,k} = -r_{i-k} b_{s,i-k} V_i V_k \cos\left(\theta_{i-k} + \gamma_{se,i-k}\right) \tag{5}$$

$$Q_{inj,k} = -r_{i-k} b_{s,i-k} V_i V_k \sin\left(\theta_{i-k} + \gamma_{se,i-k}\right) \tag{6}$$

At any operating condition, the amount of rear power imparted to the DC link is shared to the series converters and hence the GUPFC operating constraint is:

$$P_{inj,i} - \sum_n P_{inj,n} = 0, \ n = j, k \tag{7}$$

2.2 OUPFC

The basic difference between UPFC and OUPFC can be understood by comparing Fig. 2a and b respectively. Generally UPFC consists of shunt converter coupled with excitation transformer and series converter coupled with injecting transformer as shown in Fig. 2a. A similar configuration can be found in Fig. 2b for OUPFC except the transformers with triple winding. The secondary windings of these two transformers are connected by a PST which can controlled by static/mechanical switches to inject a voltage with fixed phase into the transmission line. On the other side, the tertiary windings of these two transformers are used for conventional UPFC configuration.

According to PIM of OUPFC, the injection powers at bus *i* and bus *j* are given as follows:

$$\begin{aligned} P_{inj,i} = &-b_{se} a V_i V_j \sin\left(\theta_i - \theta_j + \alpha_{pst}\right) \\ &- b_{se} r V_i V_j \sin\left(\theta_i - \theta_j + \gamma_{upsc}\right) \end{aligned} \tag{8}$$

$$\begin{aligned} Q_{inj,i} = &-b_{se} V_i^2 \left(a^2 + r^2\right) - 2 b_{se} a r V_i^2 \cos\left(\alpha_{pst} - \gamma_{upsc}\right) \\ &- 2 b_{se} V_i^2 \left\{a \cos\left(\alpha_{pst}\right) + r \cos\left(\gamma_{upsc}\right)\right\} \\ &+ b_{se} V_i V_j \left\{ \begin{array}{c} a \cos\left(\theta_i - \theta_j + \alpha_{pst}\right) \\ + r \cos\left(\theta_i - \theta_j + \gamma_{upsc}\right) \end{array} \right\} \end{aligned} \tag{9}$$

$$P_{inj,j} = -P_{inj,i} \tag{10}$$

Fig. 1 **a** Single line diagram of IPFC. **b** Single line diagram of GUPFC

(a) Single line diagram of IPFC

(b) Single line diagram of GUPFC

Fig. 2 **a** Single line diagram of UPFC. **b** Single line diagram of OUPFC
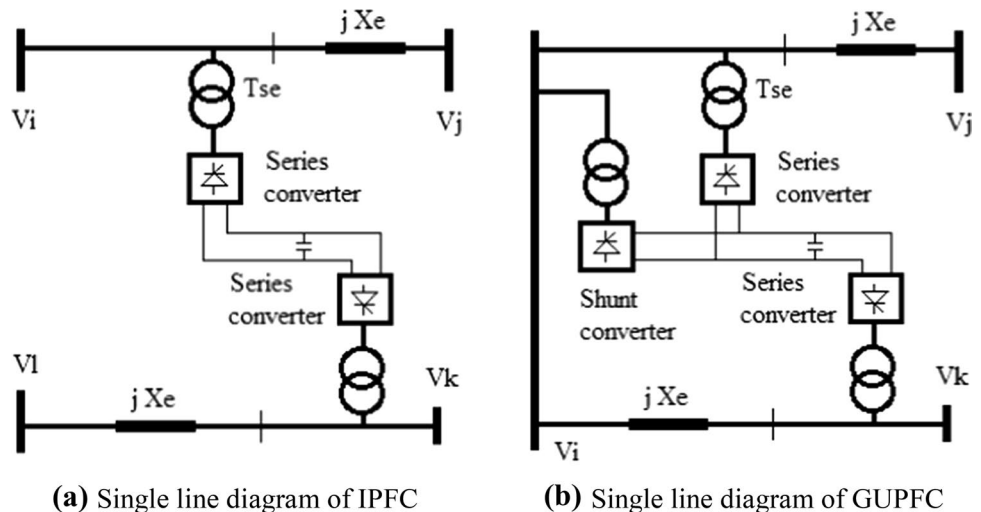
(a) Single line diagram of UPFC

(b) Single line diagram of OUPFC
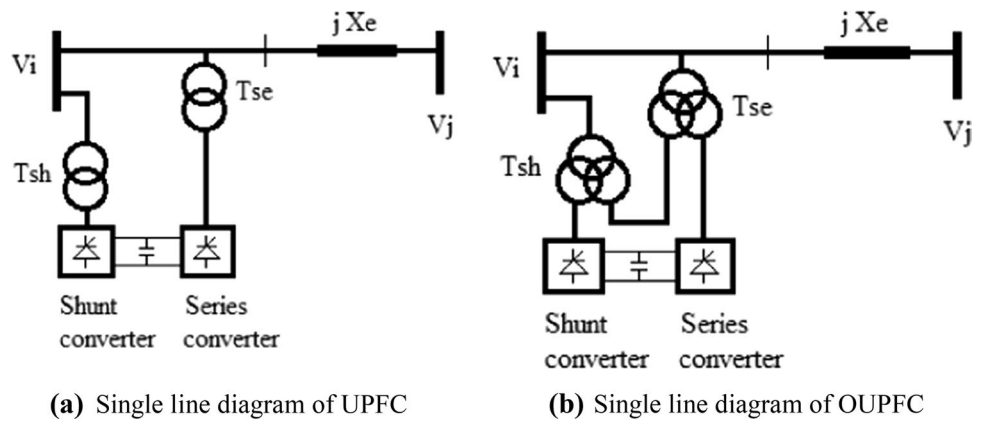
$$Q_{inj,j} = b_{se} V_i V_j \left\{ \begin{array}{c} a \cos \left(\theta_i - \theta_j + \alpha_{pst} \right) \\ + r \cos \left(\theta_i - \theta_j + \gamma_{upsc} \right) \end{array} \right\} \quad (11)$$

2.3 Optimal Location

The dependency of voltage stability on reactive power reserve in the network is well highlighted fact in the literature. Basically FACTS devices are passive in nature and can be able to redistribute the reactive power flows in the network by acting either reactive power source or sink. Our aim is to validate the FACTS devices support more on reactive power control by assessing system security which can highlight their presence in the network significantly.

To enhance the power system performance in terms of reduced transmission loss, improved voltage profile as well security margin, it is necessary to integrate the FACTS in an optimal location. In this paper, a methodology based static security measure using Line Stability Index (LSI) [26] is proposed. For a transmission line connected between bus-*p* and bus-*q*, LSI can be assessed by Eq. (12).

$$LSI_{pq} = \frac{4 x_{pq} Q_{qp}}{\left\{ \left| V_p \right| \sin \left(\theta_{pq} - \delta_p + \delta_q \right) \right\}^2} \le 1.00 \quad (12)$$

For stable operation, the LSI should be less than 1 for all the lines. The LSI greater than 1 indicates the proximity of instability or voltage collapse. The stability or security margin improvement can be shown by decreasing the LSI of all the lines. By observing the parameters in LSI, it is directly proportional to reactive power flow through the line and inversely proportional to the square of the voltage magnitude. Since the FACTS devices are able to control the reactive power flows as well as improve the voltage profile, the location which can moderate the LSI value of all the lines is selected as optimal location for the FACTS devices. Also, the stressful condition of all the line from its LSI value can be used to identify/rank the critical lines

in network. In this work, the lines which are not having regulating transformers as well as not incident to generator/synchronous condenser buses are only considered for the FACTS devices integration.

3 Problem Formulation

The overall objective function is formulated based on considering two performance indices under the conditions of different RES penetration levels as discussed here.

3.1 Consideration of RES Intermittency

In this work, it is assumed that the total installed capacity of RESs across network should not be more than total connected load of the network, hence, the total RES installed capacity IC_{res} is given by;

$$IC_{res} = \lambda_t \sum_{i=1}^{nb} P_{d,i} \quad (13)$$

In general, any types of RES may not produce always at its maximum capacity due to dependency on various parameters involved in their operation. For example, wind turbine power is dependent on wind velocity and solar PV system generation is dependent on solar radiation etc. Hence, it is assumed that the power generated by any RES is less than its maximum capacity. In addition, it is also assumed that the installed capacity of RES at a bus should not be more than connected load of that bus for avoiding reverse flows in the network. By considering these assumptions, a random number ($r_{int,i}$) will be adjusted optimally for all the RES buses in the range of ($0 \le r_{int,i} \le \lambda_t$). The power generation at a RES bus ($r_{int,i} P_{d,i}$) and correspondingly percentage of total RES intermittency ($\%In_{res}$) in the network is determined as:

$$\%In_{res} = \left(\sum_{i=1}^{nbr} r_{\text{int},i} P_{d,i} \Big/ IC_{res} \right) \times 100 \tag{14}$$

3.2 Objectives Formulation

Due to the dependency of transmission system security on voltage profile, it is essential to maintain adequate voltage profile across the network for having sufficient security margin. In this paper, the performance indices such as average voltage deviation index (AVDI) and total real power loss are taken for formulation of overall objective function.

3.2.1 Average Voltage Deviation Index (AVDI)

Considering slack bus voltage as reference, the average voltage deviation index (AVDI) is expressed as given in Eq. (15). Minimization of AVDI can ensure proper voltage profile across the network and consequently sufficient voltage stability margin in the system.

$$f_1 = AVDI = \frac{1}{nb} \sum_{i=1}^{nb} \left(\frac{|V_{i,ref}| - |V_i|}{|V_{i,ref}|} \right)^2 \tag{15}$$

3.2.2 Real Power Loss

The optimization problem is formulated to maximize transmission system stability and minimize real power loss. Mathematically,

$$\begin{aligned} f_2 = P_{loss} &= \sum_{k=1}^{nl} I_k^2 r_k \\ &= \sum_{i=1}^{nb} \sum_{\substack{j=1 \\ j \neq i}}^{nb} \left\{ Y_{ii} \cos \theta_{ii} \left[V_i^2 + V_j^2 - 2V_i V_j \cos \left(\delta_{ij} \right) \right] \right\} \end{aligned} \tag{16}$$

3.3 Overall Objective Function

The overall objective function (OOF) is formulated to minimize average voltage deviation index, AVDI (f_1), and total real power loss P_{loss}, (f_2) simultaneously and expressed as,

$$OOF = \min(f_1 + f_2) \tag{17}$$

3.4 Operational Constraints

The above objective function is optimized by satisfying the following Equality and In-equality constraints.

3.4.1 Equality Constraints

As per load flow studies, the residual powers at any bus should be equal to generation minus demand. Here, generation is expressed in terms of CES and RES powers. Power flow equations corresponding to both real and reactive power balance equations are the equality constraints that can be written, for all the buses expect FACTS incident buses, as

$$\begin{aligned} P_i &= \sum_{k=1}^{nb} |V_i||V_k||Y_{ik}| \cos \left(\theta_{ik} - \delta_i + \delta_k \right) \\ &= \left(P_{gi} + r_{\text{int}} P_{gi,r} \right) - P_{di} \quad i = 1, 2, \dots, nb \end{aligned} \tag{18}$$

$$\begin{aligned} Q_i &= - \sum_{k=1}^{nb} |V_i||V_k||Y_{ik}| \sin \left(\theta_{ik} - \delta_i + \delta_k \right) \\ &= \left(Q_{gi} + r_{\text{int}} Q_{gi,r} \right) - Q_{di} \quad i = 1, 2, \dots, nb \end{aligned} \tag{19}$$

where P_{gi} & P_{di}, Q_{gi} and Q_{di} are the real and reactive power generations and loads at bus i respectively; r_{int} is the random numbers in the range of [0, 1] to represent the intermittence of the RES at bus i related to maximum real power $P_{gi,r}$ and reactive power generations $Q_{gi,r}$ respectively. For the buses which are CES, r_{int} is to be considered as zero.

Similarly, for the FACTS incident buses, the real and reactive power balance equations can be written as,

$$\begin{aligned} P_i &= P_{g,i} - \left(P_{d,i} + P_{inj,i} \right) \\ &= \sum_{k=1}^{nb} |V_i||V_k||Y_{ik}| \cos \left(\theta_{ik} - \delta_i + \delta_k \right) \end{aligned} \tag{20}$$

$$\begin{aligned} Q_i &= Q_{g,i} - \left(Q_{d,i} + Q_{inj,i} \right) \\ &= - \sum_{k=1}^{nb} |V_i||V_k||Y_{ik}| \sin \left(\theta_{ik} - \delta_i + \delta_k \right) \end{aligned} \tag{21}$$

where $P_{inj,i}$ and $Q_{inj,i}$ are the real and reactive power injections by FACTS devices as given in Eqs. (1)–(4) and (11) for OUPFC incident buses and (5)–(11) for GUPFC.

3.4.2 Inequality Constraints

(a) Real power generation limits: this includes the upper and lower real power limit of CES.

$$P_{gi,\min} \leq P_{gi} \leq P_{gi,\max}, \ i = 1, 2, \dots, ng \tag{22}$$

(b) Reactive power generation limits: this includes the upper and lower reactive power limit of CES.

$$Q_{gi,\min} \leq Q_{gi} \leq Q_{gi,\max}, \ i = 1, 2, \dots, ng \tag{23}$$

(c) Voltage limits: this includes the upper and lower limits on the bus voltage magnitude.

$$\left| V_i^{\min} \right| \leq |V_i| \leq \left| V_i^{\max} \right|, \ i = 1, 2, \ldots, nb \tag{24}$$

(d) Phase angle limits: this includes the upper and lower limits on the bus voltage phase angle.

$$\delta_i^{\min} \leq \delta_i \leq \delta_i^{\max}, \ i = 1, 2, \ldots, nb \tag{25}$$

(e) Tap-Changers limits: this includes the upper and lower limits on the tap positions in tap-changing transformer lines.

$$a_i^{\min} \leq a_i \leq a_i^{\max}, \ i = 1, 2, \ldots, ntcl \tag{26}$$

(f) MVAr injection limits: this includes the upper and lower limits on the MVAr injections at voltage controlled buses.

$$Q_{c,inj,i}^{\min} \leq Q_{c,inj,i} \leq Q_{c,inj,i}^{\max}, \ i = 1, 2, \ldots, nvcb \tag{27}$$

(g) Line flow limits: These constraints represent the maximum MVA power flow in a transmission line.

$$|S_l| \leq \left| S_l^{\max} \right|, \ l = 1, 2, \ldots, nl \tag{28}$$

4 Cuckoo Search Optimization

This section presents the optimization procedure for FACTS parameters under various RES penetration levels by using basic Cuckoo Search Algorithm (CSA) and its three variants.

4.1 Overview of CSA

Cuckoo Search Algorithm (CSA) is one of the recent nature-inspired algorithms introduced by X. S. Yang in 2009 which inspired by brood reproductive strategy of Cuckoo birds to increase their population and it is more effective than other same family algorithms such as bat-inspired algorithm (BIA), differential evolution (DE), simulated annealing (SA), particle swarm optimization (PSO) and artificial bee colony (ABC) algorithms [45, 46] etc. The major difference between CSA to other similar algorithms is the balance between local random walk to global random walk by its switching parameter and hence effective in terms of convergence speed to reach global optima. The switching parameter $p_a \in [0, 1]$ used to control the balance between local and global random walk and are related mathematically as defined in Eq. (29).

$$v_i^{t+1} = v_i^t + \alpha s \otimes H(p_a - \varepsilon) \otimes \left(v_j^t - v_k^t \right) \tag{29}$$

$$v_i^{t+1} = v_i^t + \alpha L(s, \lambda) \tag{30}$$

where v_i^t and v_k^t are current position selected by random permutation; α is positive step size scaling factor; s is step size; H is heavy-side function; p_a is switching parameter between local and global random walk; ε is random number from uniform distribution; $\otimes$ is entry-wise product of two vectors; $L(s, \lambda)$ is Levy distribution, used to define the step size of random walk.

Lévy flights essentially provide a random walk while their random steps are drawn from a Lévy distribution for large steps. One of the effective methodologies to generate step size is using Mantegnas equations using gamma distribution function, $\Gamma()$, described by;

$$\lambda = \left| \frac{\left[\Gamma(1 + \beta) \cdot \sin\left(\frac{\pi \beta}{2} \right) \right]}{\left[\Gamma\left(\frac{1+\beta}{2} \right) \cdot \beta \cdot 2^{\left(\frac{\beta-1}{2} \right)} \right]} \right|^{1/\beta}; \ \beta = \frac{3}{2}; \tag{31}$$

$$u = rand().\alpha; \ u = rand(); \ s = \frac{u}{|v|^{\frac{1}{\beta}}}. \tag{32}$$

Precisely, the improvements for CSA towards better efficiency have been addressed by various researcher using different probability distributions for defining the step size of random walk and dynamically adjustment for switching parameter between local and global random walks. In [47], Gauss distribution based CSA has proposed and results have shown the Gauss-CSA outperformed than originally Levy-CSA in terms of higher convergence rate with reduced average generation. In [48], Gaussian and Cauchy distributions have been proposed and proved their superiority than Levy-CSA by applying to the web documents clustering problem. Similarly Cauchy distribution based CSA also in [49], and has applied for solving the economic emission load dispatch problem with multiple fuels options but the results have shown Levy-CSA is better than other Gaussian-CSA and Cauchy-CS by having lesser computational time. In [50, 51], Gamma distribution based CSA has been proposed and proved the Gamma-CSA superiority than Levy-CSA in terms of accuracy and average time. On other side, lineally decreasing switching parameter instead of constant switching parameter in original CSA in [52] and sorting function instead of permutation [53] have been proposed for better efficiency. In addition, the reader can found some other significant literature on CSA improvements in [37].

This paper adopted the recent improvement of CSA i.e., (i) linearly decreasing switching parameter, (ii)

exponentially increased switching parameter and (ii) increased switching parameter in a power of three as iteration increases [37]. Mathematically,

For linearly increased switching parameter,

$$p_a^{(k)} = p_{a,\max} \times \frac{k}{k_{\max}} \tag{33}$$

For exponentially increased switching parameter,

$$p_a^{(k)} = p_{a,\max} \times \exp\left(\frac{k}{k_{\max}}\right) \tag{34}$$

For increased switching parameter in a power of three,

$$p_a^{(k)} = p_{a,\max} \times \left(\frac{k}{k_{\max}}\right)^3. \tag{35}$$

This paper used the notation CSA_0 for the original CSA [37], CSA_1 for linearly increased switching parameter, CSA_2 for exponentially increased switching parameter, CSA_3 for increased switching parameter in a power of three.

4.2 Solution Approach Using CSA

The overall procedure for solving the proposed fitness function is described here.

4.2.1 Vector of Control Variables

This paper is aimed to minimize the voltage deviation w.r.t. reference voltage, real power loss and line stability index under RES uncertainty by optimizing the FACTS parameters. All these objectives are highly dependent on adequate voltage profile which can achieve by having optimal controls of the FACTS devices. Hence, the vector of control variables consists of generator bus voltage magnitudes, tap-changer settings, shunt MVAr injection, control variables of FACTS devices and generations at RES locations. For the GUPFC, the control variables are voltage magnitudes and their angles of two series VSCs where as for OUPFC, UPFC voltage source magnitude and its angle as well as PST voltage regulation and its angle.

4.2.2 Fitness Function

In each iteration, the system bus data and line data is updated with new population comprises generator bus voltage magnitudes, tap-changer ratios, shunt MVAr injections, controlling variables of FACTS devices (voltage magnitudes and angles) and correspondingly power injections at their incident buses and generation at RES locations. By having NR power flow solution, average voltage deviation index, total active power losses and average line stability index are computed to update the overall objective function expressed in Eq. (15). We consider the weighting factor $w_i = 1$ to have equal priority of each objective function. The solution that minimizes the overall objective function is considered the best solution.

4.2.3 Overall Procedure

1. Read system bus data, line data, type of FACTS device (OUPFC/GUPFC), IC_{res} level (λ_t) and CSA controlling parameters such as number of nests (n_{nest}), probability rate (p_a) and maximum iterations (it_{max}).
2. Determine no. buses (n_{bus}), no. generator buses (n_{gen}), no. of lines (n_{line}), no. of tap-changers (n_{tap}), no. of shunt MVAr locations (n_{shunt}), no. of load buses for RES locations (n_{res}).
3. By assuming RES penetration level as zero, perform load flow using NR method. Store the results as base case and compute voltage profile, total real power loss, LSI of all the lines and AVDI.
4. Rank the lines as per LSI value and choose the line(s) for FACTS integration. As per the power flow direction, decide line incident buses as i and j for OUPFC and i, j and k for GUPFC.
5. Define the upper and lower limits of various control variables (v_c) i.e., generator bus voltage magnitudes in the range of [0.9, 1.1] and size of ($n_{nest} \times n_{gen}$), tap-changer settings in the range of [0.95, 1.05] and size of ($n_{nest} \times n_{tap}$), shunt MVAr injections in the range of [− 100, 100] and size of ($n_{nest} \times n_{shunt}$), controlling variables of FACTS devices namely series VSC voltage in the range of [0, 0.2] and size of ($n_{nest} \times n_{se}$), series converter angles in the range of [− pi, + pi] and size of ($n_{nest} \times n_{se}$), and PST angles in the range of [− pi, + pi] and size of ($n_{nest} \times 1$), and generations at RES locations in the range of [0, λ_t] and size of ($n_{nest} \times n_{res}$).
6. Generate randomly initial population or nests. $nest(i, :) = LB + (UB - LB) \otimes rand(v_c)$ for n_{nest} times.
7. Evaluate fitness function value given in (17) after NR method load flow, by modifying the bus data with FACTS injections, RES powers, generator bus voltages, shunt injections and line data with tap-changer values.
8. Determine the best fitness and best nest, set iteration count $it_n = 1$.
9. Create Cuckoo eggs via Levy flight, using Eqs. (31) and (32), and new nests (29) and (30). Modify the eggs that violate the limits as defined at (5).
10. Determine new fitness values for all the new nets created at (9) and compare with (8) to update best fitness and best nest, set iteration count $it_n = it_n + 1$.

11. Discovery alien-Cuckoo eggs by random biased walks using switching parameter described in (33) to (35) as per the type of CSA algorithm and create new nests.

12. Repeat (9)–(11) until $it_n = it_{max}$ and stop.

5 Results and Discussions

The proposed approach is applied on standard IEEE test systems. The test systems data is taken from [54]. The simulation studies were carried out on Intel core i5 CPU@2.50 GHz system (personal computer) in MATLAB 7.8 environment.

In FACTS modeling, the leakage reactance of the exciting and injecting transformers is neglected. The radius of the OUPFC and GUPFC is considered in the range [0.0, 0.2 p.u], phase angle range as [− 180°, + 180°] and all the generator bus voltages are regulated in the range of [0.9 p.u., 1.1 p.u].

The CSA parameters considered in this paper are: the number of nests = 25; the discovery rate of alien eggs/solutions, Pa = 0.25; In TVAC-PSO, no. of population = 50; $C_{1max} = 2$; $C_{1min} = 0.4$; $C_{2max} = 0.4$ and $C_{2min} = 2$ and no. are considered [55]. For both the algorithms, no. of maximum iterations considered as 50. From the fitness function, function, 'f_1' is to be considered as percentage AVDI and function 'f_2' is to be considered as Total Real Power Loss in MW.

5.1 Optimal Location

The proposed methodology for finding optimal location of OUPFC and GUPFC is applied on IEEE 14-, 30- and 57-bus test systems. At first, the LSI values are determined for all the lines in each system and the lines are ranked in descending order. By excluding the lines which are incident to generator buses as well as those are having tap-changing transformer, the top 5 ranked lines as per LSI values associated with line number are given in Fig. 3 for all the test systems.

In 14-bus system, line # 17 (9–14) is ranked first with LSI value of 0.436 and chosen for OUPFC integration. Similarly, line # 38 (27–30) with LSI value of 0.0511 and line # 78 (38–49) with LSI value of 0.1039 are chosen for OUPFC in 30–bus and 57–bus system respectively. For the GUPFC, two top ranked lines with one bus as common are chosen as optimal locations. In 14–bus, line # 17 (9–14) & line # 20 (13–14) are chosen. In 30-bus, line # 38 (27–30) and line # 37 (27–29) are considered. Similarly line # 78 (38–49) and line # 50 (37–38) are considered in 57-bus system.

5.2 Optimal Parameters of FACTS Devices

In this section, it is assumed that all the load buses in the test system are integrated with a RES and objective function is solved by proposed CSA variants. Their capacity will be considered as an input to the program for every case study. For an example a 10% of total load is assumed to be supplied by all the RES across the network, then λ_t will be equal to 0.1. For different values of r_{int} ($0 \leq r_{int,i} \leq \lambda$) at different RES locations, the total power supplied may or` not equal to RES installed capacity. The ratio of total RES generation to RES installed capacity is considered as the percentage of RES intermittency. The case studies for IEEE 14-, 30- and 57-bus are presented in this section and these are further divided into three categories, (i) Case A: RES capacity of 10%, (ii) Case B: RES capacity of 20%, and (iii) Case C: RES capacity of 30%.

Fig. 3 Top 5 ranked lines as per LSI values in each system
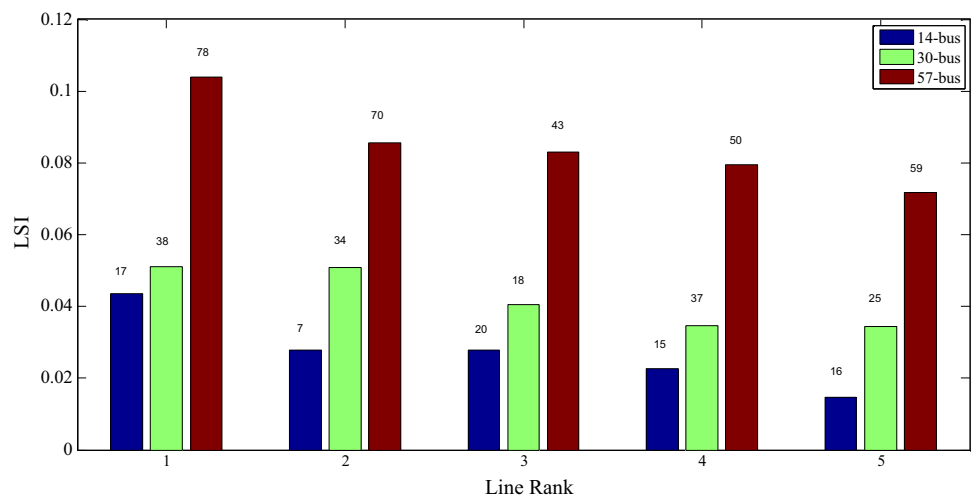
5.2.1 14-Bus System

The system consists of 5 generator buses and 9 load buses interconnected by 20 transmission lines. The system has 259 MW real and 73.5 MVAr reactive power load. A 40 MW generation is scheduled at bus 2 and the remaining load is supplied by slack bus 1. It is observed that the test system is suffering with 13.393 MW real and 54.54 MVAr reactive losses using NR load flow. In addition, it is observed that the system have AVDI, $f_1 = 0.0031$, P_{loss}, $f_2 = 13.3933$, and correspondingly $OOF = 13.3964$ for this base case operating condition.

As determined in Sect. 5.1, line # 17 (9–14) is modeled for OUPFC for power injections at bus-9 (i) and bus-14 (j). Similarly for GUPFC locations line # 17 (9–14) & line # 20 (13–14), the power injections are done at bus-14 (i), bus-9 (j) and bus-13 (k) respectively.

In optimization problem, the test system has 23 variables related to 5 generator bus voltages, 9 RES locations, 3 tapchangers, 1 shunt VAr injections, 5 parameters in FACTS modeling (2 series voltage magnitudes, 2 series voltage angles and 1 shunt VAr injection). The optimized values of various parameters involved in optimization problem considering OUPFC in the system are determined by proposed CSA variants are tabulated in Table 1. From this table, it is observed that CSA3 is outperformed among all other variants including TVAC-PSO. As compared with base case, the objective function f_1 and f_2 are decreased for all the algorithms at all the RES intermittency levels. In addition, it can also be concluded that the affect of RES intermittency on system performance is also significantly controlled by OUPFC controls by having decreased losses and improved voltage profile at all the cases.

Similarly, the results for GUPFC are given in Table 2. As observed in OUPFC results, the GUPFC is also capable of mitigating the impact of RES intermittency on system performance. But the OUPFC has shown better results than GUPFC by providing improved voltage profile and reduced losses in the network.

In all the cases, the decreased OOF value by CSA_3 is shown the effectiveness of dynamic switching parameter than fixed as used in CSA_0. On the other side, it is observed that the TVAC-PSO is also competitive with CSA_0, CSA_1 and CSA_2 in all the cases. In addition, the convergence time of all the algorithms is also given in the same table. By observing the convergence time also, it can be concluded that CSA_3 is faster than remaining algorithms in all the cases. The convergence characteristics for the Case-C and for OUPFC and GUPFC are shown in Figs. 4 and 5 respectively. The performance of OUPFC and GUPFC interms of AVDI and P_{loss} for IEEE 14 bus system under different RES intermittency conditions is shown in Fig. 6. The overall objective function and the corresponding convergence time are shown in Fig. 7.

5.2.2 30-Bus System

In this test system, there are 6 generator buses (i.e., 1, 2, 5, 8, 11 and 13), 24 load buses interconnected by 41 transmission lines. It has 283.40 MW real and 126.20 MVAr reactive loads. The system is suffering with 17.557 MW real and 67.69 MVAr reactive power losses for a generation schedule of 40 MW at bus 2 and the remaining load is supplied by slack bus 1. The objective functions for this operating condition are AVDI, $f_1 = 0.0054$, P_{loss}, $f_2 = 17.557$ and $OOF = 17.5623$.

**Table 1** Optimized OUPFC parameters in 14-bus system for different $\%In_{res}$

Case	Algorithm	$\%In_{res}$	$P_{inj,i}$	$Q_{inj,i}$	$P_{inj,j}$	$Q_{inj,j}$	F_1	F_2	OOF	Time (s)
A	CSA0	63.020	33.291	− 35.152	− 33.291	30.181	0.0017	11.930	11.931	7.312
	CSA1	57.900	34.073	18.040	− 34.073	− 19.858	0.0019	11.831	11.832	6.018
	CSA2	69.690	12.358	−− 62.347	− 12.358	53.223	0.0015	11.807	11.808	6.522
	CSA3	64.960	− 2.561	− 77.664	2.561	64.530	0.0015	11.738	11.739	5.862
	TVAC	78.250	− 95.785	− 3.300	95.785	− 24.091	0.0007	11.885	11.886	6.404
B	CSA0	73.450	12.460	− 232.494	− 12.460	160.971	0.0018	11.371	11.373	6.105
	CSA1	76.640	− 19.096	− 34.511	19.096	29.502	0.0015	11.370	11.371	6.491
	CSA2	65.170	− 74.166	17.966	74.166	− 36.688	0.0017	10.899	10.900	8.244
	CSA3	59.660	− 60.307	− 6.927	60.307	− 4.470	0.0017	10.545	10.547	6.002
	TVAC	72.730	− 55.452	19.049	55.452	− 30.070	0.0008	11.273	11.274	6.542
C	CSA0	73.819	19.459	− 12.420	− 19.459	11.447	0.0029	11.008	11.011	5.900
	CSA1	65.838	− 35.893	− 86.549	35.893	67.702	0.0005	10.105	10.105	6.347
	CSA2	61.518	− 31.491	− 22.953	31.491	17.739	0.0009	9.823	10.029	6.013
	CSA3	68.281	4.386	2.597	− 4.386	− 2.396	0.0014	10.028	9.824	5.789
	TVAC	59.819	12.177	− 96.800	− 12.177	78.360	0.0026	9.888	9.891	6.053

Table 2 Optimized GUPFC parameters in 14-bus system for different %In_{res}

Case	Algorithm	%Inres	Pinj,i	Qinj,i	Pinj,j	Qinj,j	Pinj,k	Qinj,k	F1	F2	OOF	Time (s)
A	CSA0	67.212	39.740	− 72.488	− 0.601	31.446	− 39.139	41.647	0.0009	12.448	12.449	7.261
	CSA1	72.264	− 23.605	− 11.307	23.605	11.983	0.000	0.000	0.0020	12.313	12.315	6.225
	CSA2	78.129	− 13.968	10.379	18.901	− 29.145	− 4.934	18.745	0.0014	12.265	12.267	6.526
	CSA3	80.321	− 0.398	− 34.681	0.398	35.378	0.000	0.000	0.0014	11.893	11.895	6.001
	TVAC	64.866	63.810	42.501	− 23.731	− 19.517	− 40.079	− 24.767	0.0017	11.990	11.992	6.334
B	CSA0	66.367	− 7.225	4.138	7.226	− 4.175	− 0.001	0.093	0.0016	12.314	12.316	12.375
	CSA1	77.953	77.195	51.874	− 33.004	− 11.838	− 44.191	− 42.153	0.0010	12.026	12.027	6.289
	CSA2	60.409	− 11.016	− 66.674	− 1.011	52.905	12.027	15.180	0.0023	11.763	11.766	6.323
	CSA3	75.548	− 74.586	− 11.274	27.368	11.399	47.218	1.342	0.0008	11.248	11.249	6.285
	TVAC	65.203	− 31.234	− 46.025	− 0.469	24.545	31.704	22.753	0.0005	11.246	11.247	6.151
C	CSA0	68.098	44.972	− 17.011	0.000	0.000	− 44.972	16.568	0.0018	11.252	11.254	6.645
	CSA1	65.133	2.512	− 4.319	− 2.093	1.002	− 0.418	3.338	0.0009	11.121	11.122	6.009
	CSA2	74.941	34.801	20.626	18.999	− 22.050	− 53.800	0.546	0.0009	10.987	10.988	5.939
	CSA3	69.865	− 47.182	39.617	37.926	− 67.002	9.256	27.318	0.0024	10.581	10.583	5.893
	TVAC	78.112	− 12.313	76.191	− 48.802	− 64.501	61.114	− 13.127	0.0005	10.946	10.946	6.206
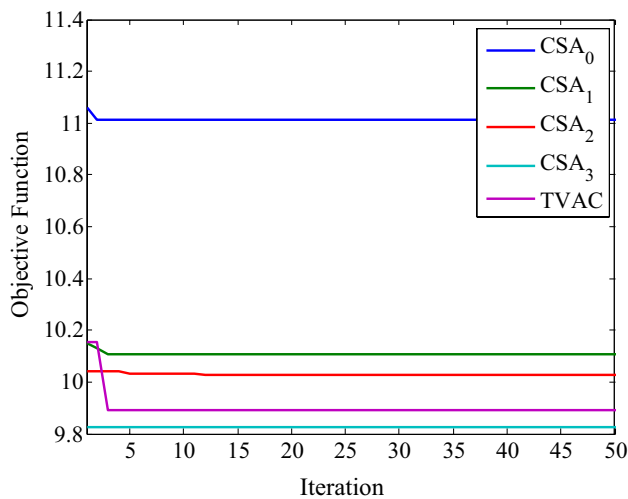
**Fig. 4** Convergence characteristics for Case—C in 14-bus test system with OUPFC
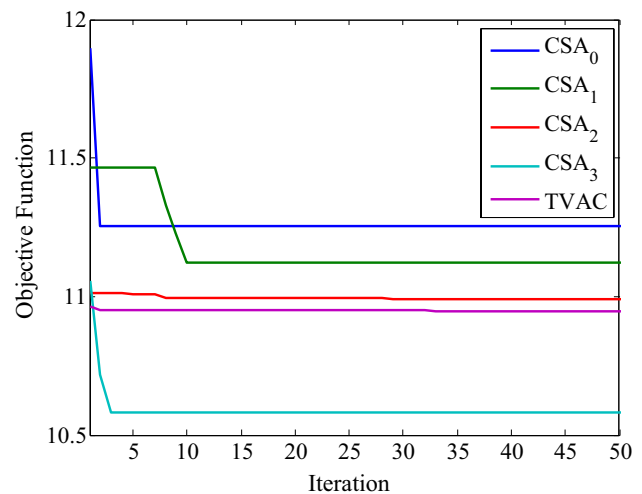
Fig. 5 Convergence characteristics for Case—C in 14-bus test system with GUPFC

As determined in Sect. 5.1, line # 38 (27–30) is modeled for OUPFC for power injections at bus-27 (*i*) and bus-30 (*j*). Similarly for GUPFC locations line # 38 (27–30) & line # 37 (27–29), the power injections are done at bus-27 (*i*), bus-30 (*j*) and bus-29 (*k*) respectively.

In optimization problem, the test system has 41 variables related to 6 generator bus voltages, 24 RES locations, 4 tap-changers, 2 shunt VAr injections, 5 parameters in FACTS modeling (2 series voltage magnitudes, 2 angles and 1 shunt VAr injection). By observing the result given in Table 3 for OUPFC, *OOF* is decreased to 15.233 for CSA3 at 10% RES installed capacity in system and correspondingly f_1 is

reduced to 0.0039 from 0.0054, which indicates the decrease in voltage deviation w.r.t. reference voltage and f_2 is reduced to 15.229 from 17.557, which indicates reduction in real power loss. The similar phenomena can be observed in Case B and Case C.

Similarly, the results for GUPFC are given in Table 4. It is observed that OUPFC has provided better results than GUPFC in all the cases. In addition, CSA3 is outperformed than remaining CSA variants as well as TVAC-PSO in terms of reduced *OOF* values as well as having less computational time. The performance of OUPFC and GUPFC in terms of AVDI and P_{loss} for IEEE
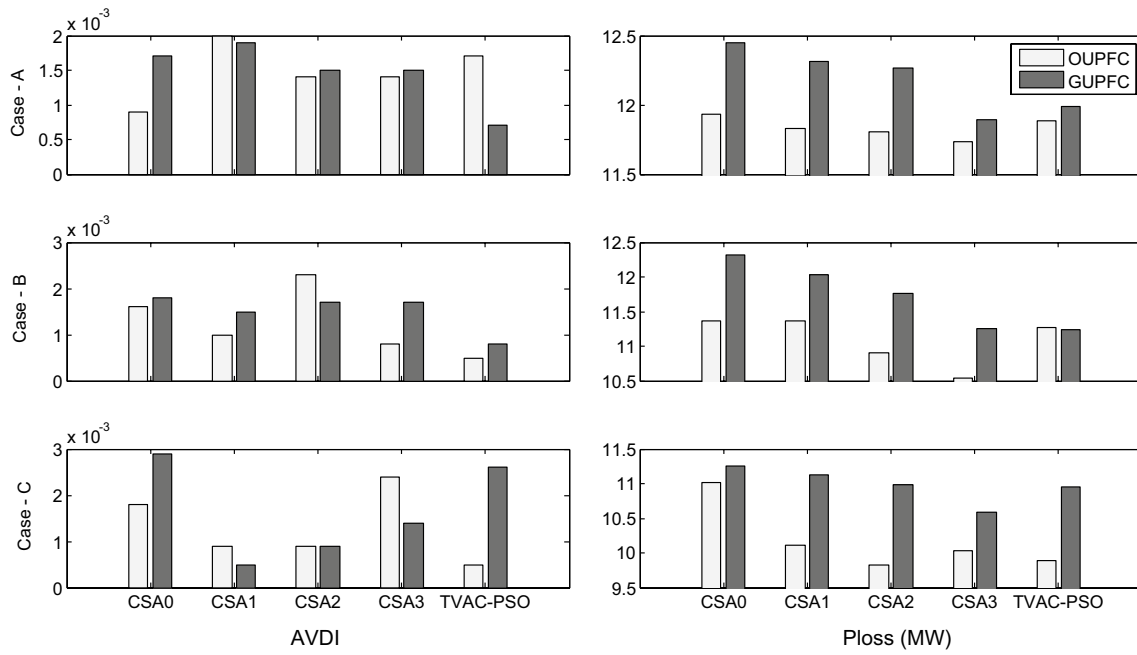
Fig. 6 AVDI and P_{loss} with OUPFC and GUPFC in 14-bus system for different RES intermittency
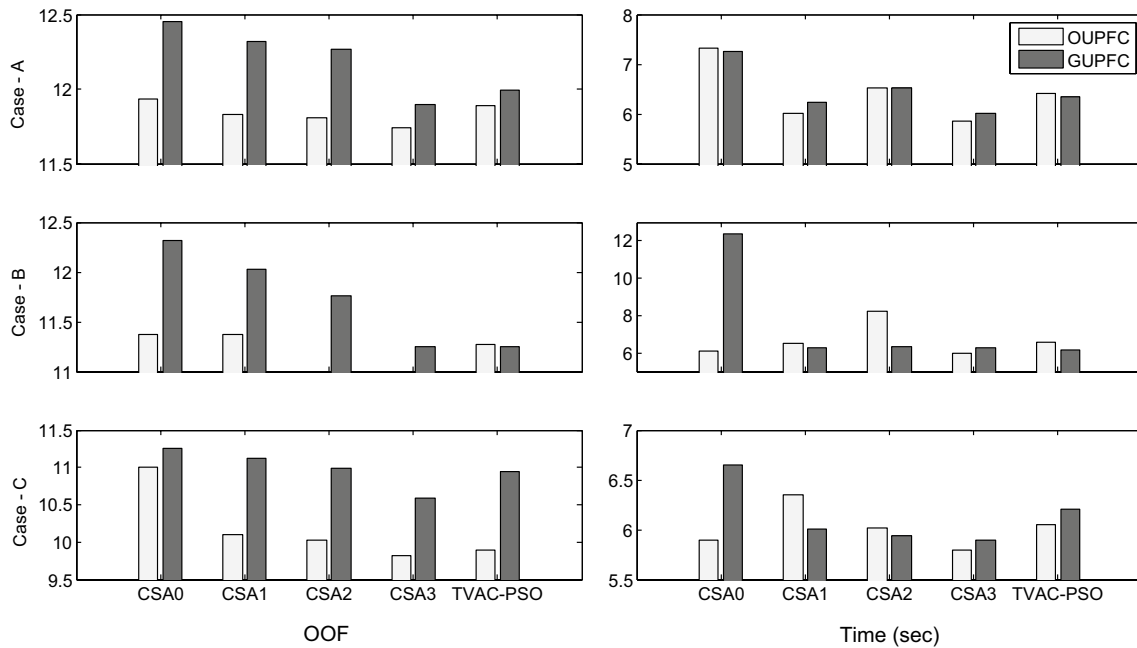
Fig. 7 The OOF and computational time with OUPFC and GUPFC in 14-bus system for different RES intermittency

30 bus system under different RES intermittency conditions is shown in Fig. 8. The overall objective function and the corresponding convergence time are shown in Fig. 9. The convergence characteristics for Case-C with OUPFC and GUPFC are shown in Figs. 10 and 11 respectively.

Table 3 Optimized OUPFC parameters in 30-bus system for different %In_{res}

Case	Algorithm	%Inres	Pinj,i	Qinj,i	Pinj,j	Qinj,j	F1	F2	OOF	Time (s)
A	CSA0	77.488	− 37.539	− 37.767	37.539	21.975	0.0038	16.045	16.049	8.394
	CSA1	79.508	14.078	14.786	− 14.078	− 15.435	0.0035	16.041	16.045	8.206
	CSA2	75.121	− 14.483	29.766	14.483	− 39.095	0.0047	15.989	15.994	8.033
	CSA3	66.842	− 11.923	14.429	11.923	− 16.913	0.0039	15.229	15.233	7.763
	TVAC	76.520	− 17.485	31.777	17.485	− 44.219	0.0027	15.529	15.532	7.633
B	CSA0	75.504	20.421	− 0.693	− 20.421	− 0.290	0.0017	15.325	15.326	9.721
	CSA1	73.938	− 17.803	26.578	17.803	− 35.334	0.0036	15.300	15.303	8.249
	CSA2	74.434	0.763	5.498	− 0.763	− 5.288	0.0030	14.881	14.884	8.119
	CSA3	73.041	0.241	7.058	− 0.241	− 6.906	0.0025	14.421	14.424	8.051
	TVAC	68.986	9.693	− 47.415	− 9.693	36.943	0.0035	14.772	14.775	8.230
C	CSA0	79.150	13.398	− 24.612	− 13.398	20.648	0.0019	14.024	14.026	8.610
	CSA1	72.761	0.273	13.279	− 0.273	− 13.546	0.0021	13.947	13.950	7.871
	CSA2	67.865	2.696	19.254	− 2.696	− 20.378	0.0019	13.840	13.842	7.699
	CSA3	71.553	4.000	− 51.953	− 4.000	39.933	0.0026	13.282	13.284	7.914
	TVAC	73.628	− 5.940	0.385	5.940	− 0.997	0.0037	13.677	13.680	7.893

Table 4 Optimized GUPFC parameters in 30-bus system for different %In_{res}

| Case	Algorithm	%Inres	Pinj,i	Qinj,i	Pinj,j	Qinj,j	Pinj,k	Qinj,k	F1	F2	OOF	Time (s)
A	CSA0	82.061	11.008	19.055	− 12.143	10.705	1.135	− 29.086	0.0040	16.855	16.859	10.584
	CSA1	75.536	31.357	− 21.619	− 11.033	11.204	− 20.324	10.724	0.0027	16.820	16.822	8.128
	CSA2	70.957	− 11.924	29.635	20.802	− 19.116	− 8.878	− 10.325	0.0035	16.621	16.624	8.076
	CSA3	70.685	23.754	− 4.742	− 19.760	8.607	− 3.994	− 3.230	0.0026	15.954	15.957	7.692
	TVAC	79.017	28.089	17.385	− 24.252	− 17.775	− 3.837	1.908	0.0027	16.295	16.298	8.123
B	CSA0	79.402	− 6.839	− 8.703	− 2.278	9.428	9.117	− 1.107	0.0045	16.457	16.461	11.214
	CSA1	77.389	1.829	− 1.311	0.637	− 0.516	− 2.466	1.837	0.0027	15.395	15.398	8.812
	CSA2	69.287	0.169	− 32.446	0.675	18.300	− 0.844	13.314	0.0027	15.307	15.310	8.811
	CSA3	80.198	− 7.065	13.411	6.419	− 13.747	0.646	0.492	0.0011	15.145	15.146	7.790
	TVAC	68.163	− 12.623	− 9.233	1.242	33.679	11.381	− 25.287	0.0029	15.214	15.217	9.378
C	CSA0	75.917	− 53.366	39.601	8.914	− 26.644	44.452	− 13.189	0.0031	15.078	15.081	10.680
	CSA1	75.474	0.708	54.151	− 12.998	− 5.944	12.290	− 46.883	0.0022	14.880	14.882	8.046
	CSA2	77.553	− 30.150	26.416	− 7.696	3.760	37.846	− 30.237	0.0017	14.607	14.609	8.173
	CSA3	65.323	− 16.821	4.358	19.637	− 1.126	− 2.815	− 3.808	0.0038	13.205	13.209	7.990
	TVAC	72.780	6.789	16.449	0.000	0.000	− 6.789	− 15.989	0.0026	14.198	14.201	7.764

5.2.3 57-Bus System

The test system consists of 7 generators buses (i.e., 1, 2, 3, 6, 8, 9 and 12) and 50 load buses interconnected by 80 transmission lines. It has 1250.80 MW real and 336.40 MVAr reactive loads. It is suffering with 27.864 MW real and 121.67 MVAr reactive power losses for a schedule of 40 MW, 450 MW and 310 MW at generator buses 3, 8 and 12 respectively. For this schedule, the system has AVDI, $f_1 = 0.0122$, P_{loss}, $f_2 = 27.8638$ and $OOF = 27.876$.

As determined in Sect. 5.1, line # 78 (38–49) is modeled for OUPFC for power injections at bus-38 (i) and bus-49 (j). Similarly for GUPFC locations line # 78 (38–49) & line # 50

(37–38), the power injections are done at bus-38 (i), bus-49 (j) and bus-37 (k) respectively.

In optimization problem, the test system has 73 variables related to 7 generator bus voltages, 50 RES locations, 9 tap-changers, 2 shunt VAr injections, 5 parameters in FACTS modeling (2 series voltage magnitudes, 2 angles and 1 shunt VAr injection). The OUPFC results are given in Table 5 and from the table, it can be observed that the OOF is decreased to 21.437, 21.085 and 17.876 in Case A, B and C respectively. Similarly, the results for GUPFC are given in Table 6. In comparison, the OUPFC has shown its flexibility than GUPFC in power flow control, voltage stability improvement and loss reduction. In addition, the CSA_3 is performed
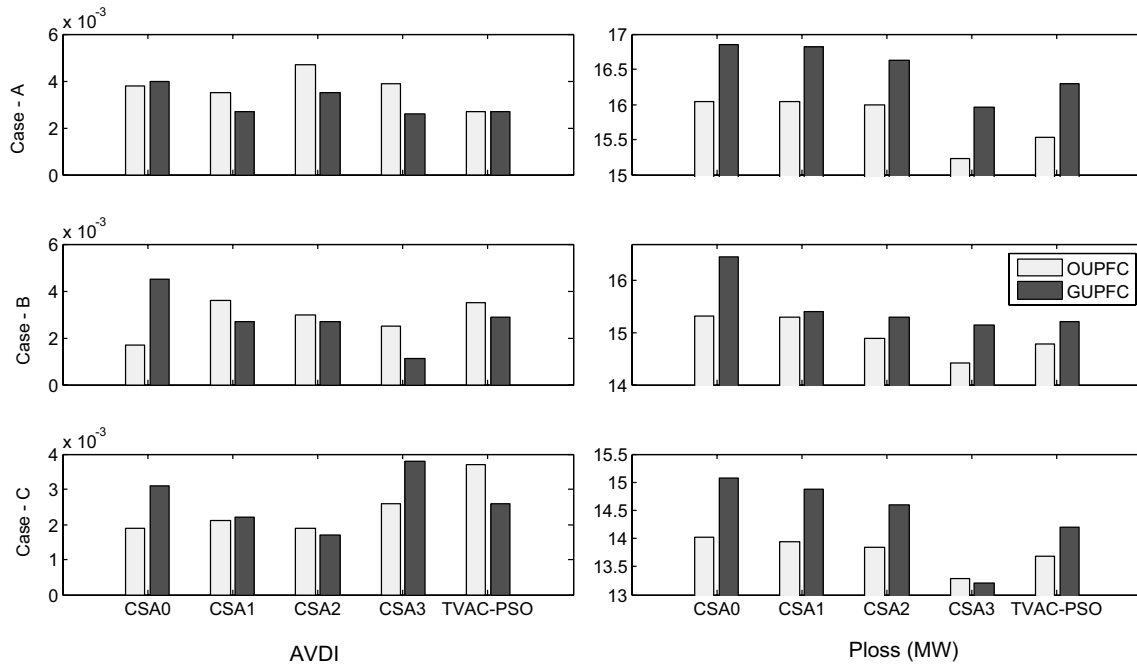
Fig. 8 AVDI and P$_{loss}$ with OUPFC and GUPFC in 30-bus system for different RES intermittency
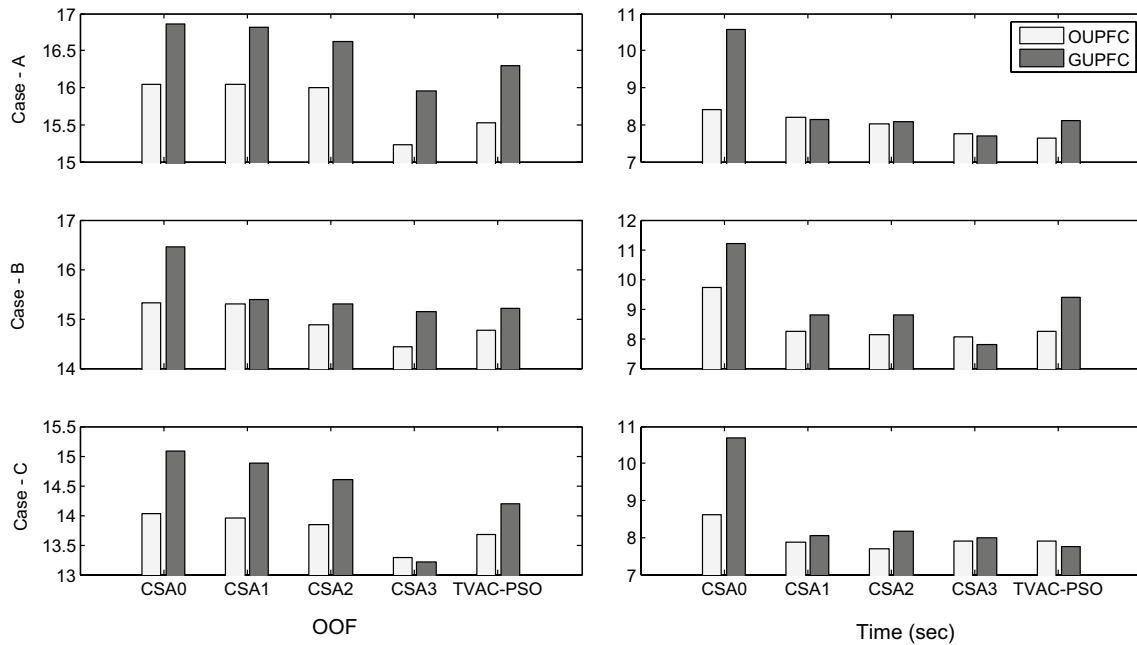

Fig. 9 The OOF and computational time with OUPFC and GUPFC in 30-bus system for different RES intermittency

better than remaining algorithms as observed in 14-bus and 30-bus test systems.

The optimized parameters for OUPFC and GUPFC devices are listed in Tables 5 and 6 respectively. From these tables it is observed that the impact of 30% RES installed capacity (Case A) is given better performance than 20%

(Case B) and 20% RES installed capacity is better than 10% RES installed capacity (Case A) integration all test systems in terms of reduced AVDI and total Real Power loss.

The performance of OUPFC and GUPFC in terms of AVDI and P$_{loss}$ for IEEE 57 bus system under different RES intermittency conditions is shown in Fig. 12. The overall
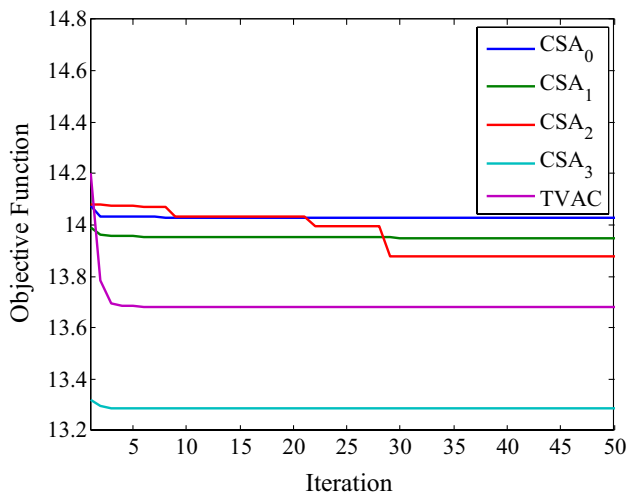
Fig. 10 Convergence characteristics for Case—C in 30-bus test system with OUPFC
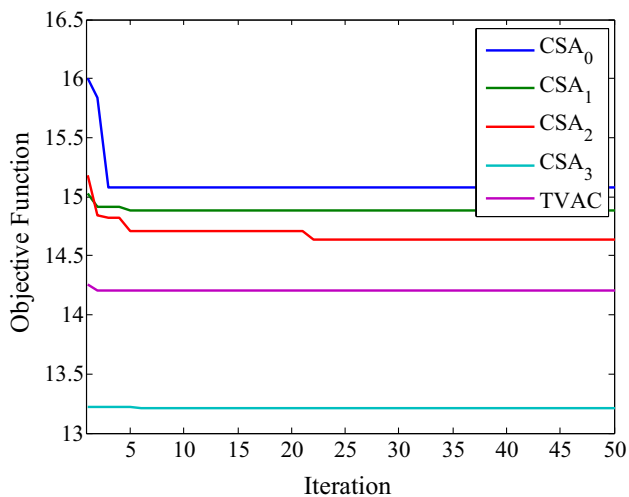
Fig. 11 Convergence characteristics for Case—C in 30-bus test system with GUPFC

objective function and the corresponding convergence time are shown in Fig. 13. The convergence characteristics for

Case-C with OUPFC and GUPFC are shown in Figs. 14 and 15 respectively.

6 Conclusion

In this paper, the impact of renewable energy sources (RES) penetration and their intermittency in modern power system operation is analyzed and proposed to moderate using optimal unified power flow controller (OUPFC) and generalized unified power flow controller (GUPFC) controls. The locations of FACTS devices are determined by using line stability index (LSI). The simulation studies on standard IEEE 14-bus, 30-bus and 57-bus test systems are highlighted the OUPFC controls than GUPFC by providing improved voltage profile and reduced losses.

The parameters involved in multi-objective problem are optimized using Cuckoo search algorithm (CSA) towards average voltage deviation index and real power loss minimization. Instead of constant switching parameter in basic CSA, three types of switching parameters i.e., linearly increased switching parameter, exponentially increased switching parameter and increased switching parameter in a power of three are proposed. From all the case studies in all the test systems, the average computational time with constant switching parameter is nearly 10.135 s, 8.769 s with linearly increased switching parameter, 8.699 s with exponentially increased switching parameter and whereas it is only 8.240 s with increased switching parameter in a power of three. On the other side, TVAC-PSO has also performed better than all other CSA variants except CSA with increased switching parameter in a power of three by having average computational time around 8.535 s. From the simulation results, it can be concluded that the CSA with increased switching parameter in a power of three outperformed than CSA with linearly increased switching parameter, exponentially increased switching parameter as well as TVAC-PSO algorithms.

Table 5 Optimized OUPFC parameters in 57-bus system for different %In_{res}

Case	Algorithm	%Inres	Pinj,i	Qinj,i	Pinj,j	Qinj,j	F1	F2	OOF	Time (s)
A	CSA0	77.350	89.417	− 103.149	− 89.417	82.987	0.0086	23.809	23.817	12.108
	CSA1	82.998	55.893	− 3.212	− 55.893	− 1.631	0.0117	23.282	23.294	11.231
	CSA2	81.558	− 38.975	− 262.501	38.975	201.758	0.0051	22.967	22.972	10.988
	CSA3	82.720	− 10.602	125.647	10.602	− 203.054	0.0083	21.429	21.437	10.886
	TVAC	85.285	− 42.786	40.624	42.786	− 50.404	0.0065	22.760	22.766	11.094
B	CSA0	79.148	9.535	− 128.565	− 9.535	112.657	0.0091	21.938	21.947	11.029
	CSA1	84.733	− 4.625	− 85.613	4.625	78.862	0.0096	21.638	21.648	10.946
	CSA2	85.334	41.389	58.422	− 41.389	− 73.067	0.0089	21.474	21.483	10.959
	CSA3	80.987	− 118.216	5.244	118.216	− 32.268	0.0032	21.081	21.085	10.860
	TVAC	82.831	− 32.412	− 146.705	32.412	124.744	0.0055	20.319	20.324	10.880
C	CSA0	76.481	− 1.457	− 23.945	1.457	24.065	0.0064	19.641	19.648	12.013
	CSA1	83.796	11.840	− 48.512	− 11.840	46.863	0.0085	19.564	19.572	11.263
	CSA2	83.806	64.287	78.542	− 64.287	− 109.720	0.0060	19.360	19.366	11.803
	CSA3	75.837	− 9.343	68.253	9.343	− 83.841	0.0057	17.870	17.876	10.916
	TVAC	83.524	180.953	− 201.190	− 180.953	127.451	0.0046	19.102	19.107	10.978

Table 6 Optimized GUPFC parameters in 57-bus system for different %In_{res}

| Case	Algorithm	%Inres	Pinj,i	Qinj,i	Pinj,j	Qinj,j	Pinj,k	Qinj,k	F1	F2	OOF	Time (s)
A	CSA0	84.431	115.433	− 69.973	− 42.833	54.137	72.600	17.635	0.0041	23.696	23.700	14.301
	CSA1	77.408	− 102.482	− 52.366	7.086	65.646	95.396	− 12.679	0.0062	23.462	23.468	11.532
	CSA2	83.370	91.737	− 93.668	81.381	9.046	− 173.118	84.371	0.0074	23.131	23.138	11.578
	CSA3	82.283	204.103	31.145	− 42.928	56.917	− 161.176	− 82.244	0.0038	21.969	21.973	10.908
	TVAC	81.917	− 40.701	12.299	11.752	− 48.982	28.949	34.198	0.0052	22.936	22.941	10.964
B	CSA0	85.818	− 73.362	30.611	− 7.649	10.602	81.011	− 40.827	0.0070	22.203	22.210	14.295
	CSA1	82.956	78.280	220.528	− 27.326	− 95.302	− 50.954	− 123.155	0.0053	22.110	22.115	12.245
	CSA2	81.216	78.369	160.990	− 30.933	− 4.209	− 47.437	− 151.870	0.0045	21.634	21.639	11.287
	CSA3	80.001	5.898	120.266	38.209	− 89.737	− 44.107	− 31.244	0.0038	20.000	20.003	10.847
	TVAC	81.262	25.419	− 33.832	− 26.571	− 62.936	1.152	92.797	0.0051	21.368	21.373	11.530
C	CSA0	82.596	− 71.040	76.159	40.866	− 68.083	30.174	− 9.862	0.0050	20.546	20.551	13.885
	CSA1	83.152	− 158.409	− 121.300	35.769	14.895	122.640	102.165	0.0044	19.302	19.307	13.950
	CSA2	79.260	162.937	196.500	− 70.163	− 83.231	− 92.774	− 110.598	0.0068	19.187	19.194	11.493
	CSA3	81.380	160.060	38.963	− 55.854	− 61.293	− 104.207	21.848	0.0068	18.248	18.255	10.876
	TVAC	76.627	− 123.906	19.558	72.436	13.715	51.470	− 32.937	0.0081	18.456	18.464	11.490
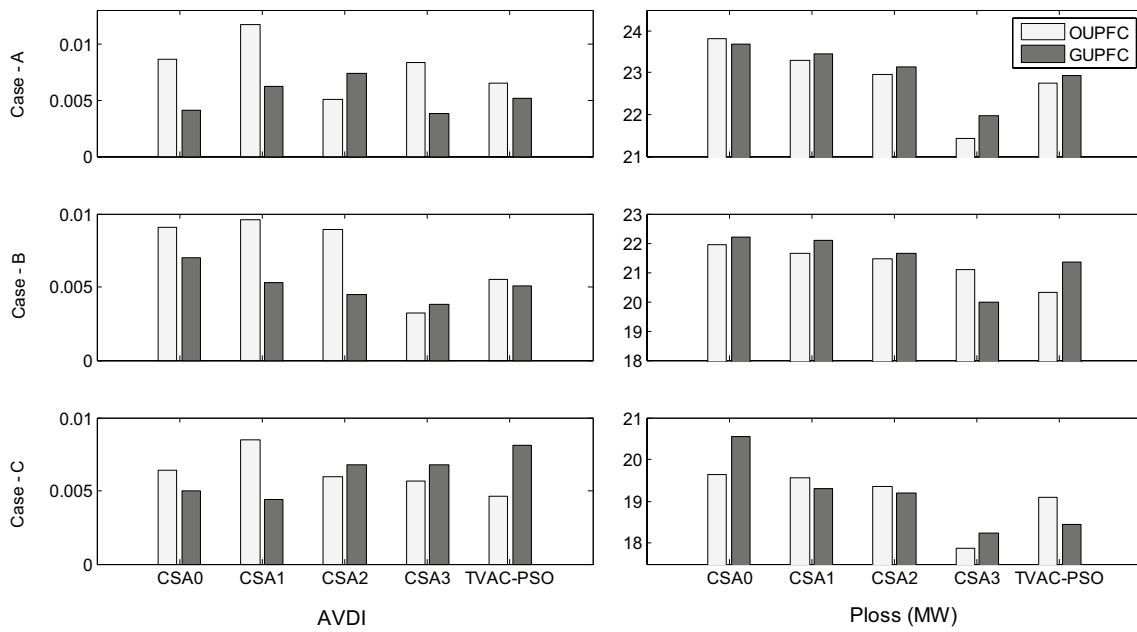
Fig. 12 AVDI and P_{loss} with OUPFC and GUPFC in 57-bus system for different RES intermittency
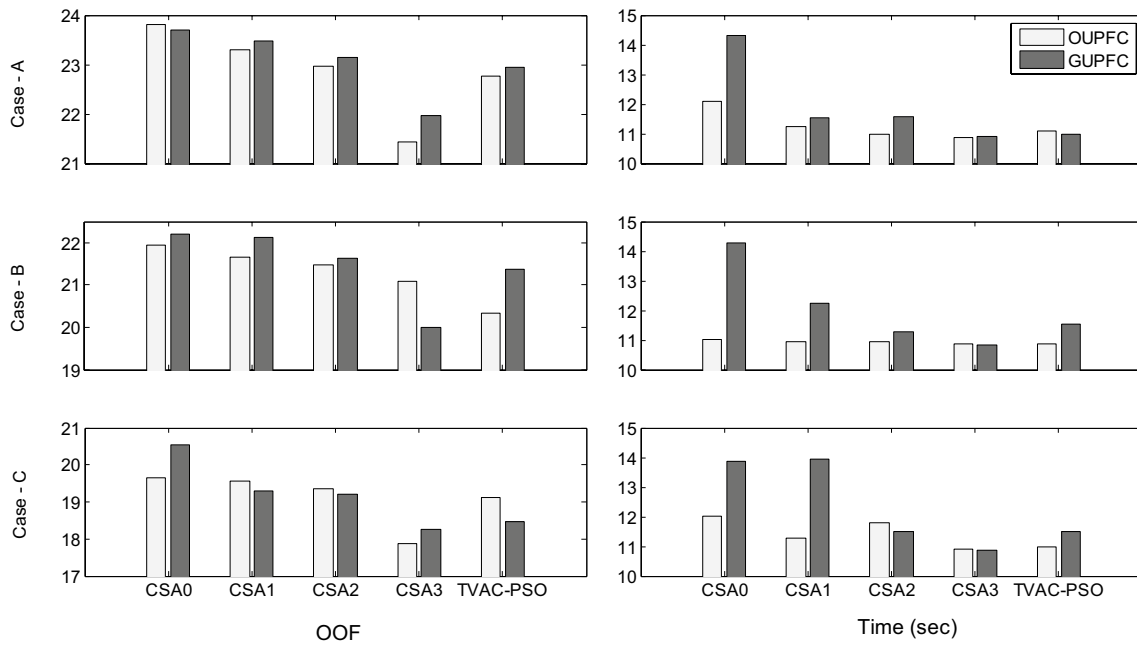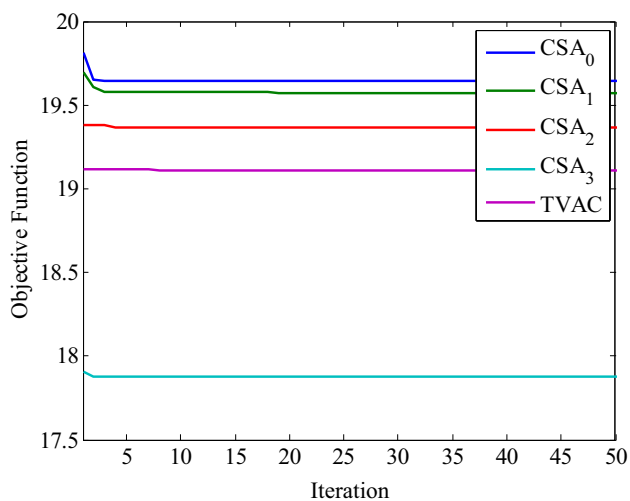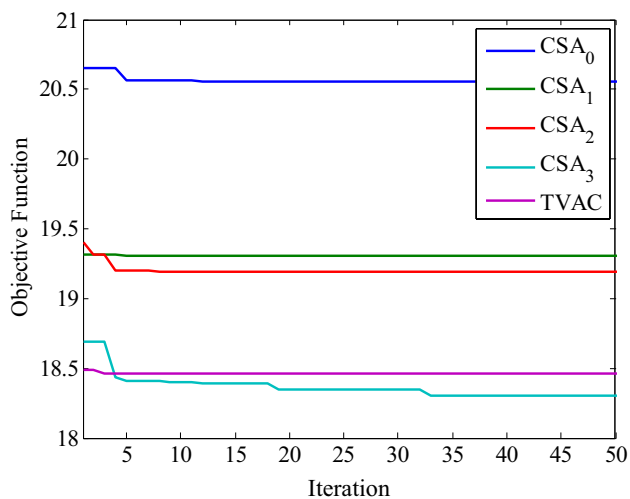

Fig. 13 The OOF and computational time with OUPFC and GUPFC in 57-bus system for different RES intermittency

Fig. 14 Convergence characteristics for Case—C in 57-bus test system with OUPFC

Fig. 15 Convergence characteristics for Case—C in 57-bus test system with GUPFC

References

1. Tagliapietra S (2018) The impact of global decarbonization policies and technological improvements on oil and gas producing countries in the Middle East and North Africa. IEMed. Mediterranean Yearbook
2. Nada KH, Alrikabi MA (2014) Renewable energy types. J Clean Energy Technol 2(1):61–64. https://doi.org/10.7763/jocet.2014
3. Adibi MM (2015) Impact of power system blackouts, v2.92. In: 2015 IEEE power & energy society general meeting, Denver, CO, July 2015. https://www.ieee-pes.org/presentations/gm2015/PESGM2015P-001079.pdf. Accessed 16 July 2020
4. Atputharajah A, Saha TK (2009) Power system blackouts—literature review. In: 2009 international conference on industrial

5. and information systems (ICIIS), Sri Lanka, pp 460–465. https://doi.org/10.1109/iciinfs.2009.5429818
5. Pikulski M (2008) Controlled sources of reactive power used for improving voltage stability. Project report, Institute of Energy Technology, Electrical Power Systems and High Voltage Engineering, Aalborg University, June 2008. https://pdfs.semanticscholar.org/5298/b641b1a7ff6eca7b 329be75c59e066bf3aca.pdf. Accessed on 16 July 2020
6. Roy PK, Ghoshal SP, Thakur SS (2012) Optimal VAR control for improvements in voltage profiles and for real power loss minimization using biogeography based optimization. Int J Electr Power Energy Syst 43(1):830–838. https://doi.org/10.1016/j.ijepes.2012.05.032
7. Hingorani NG, Gyugyi L (2000) Understanding FACTS: concepts and technology of flexible AC transmission systems. IEEE Press, New York. ISBN 978-0-780-33455-7
8. Kang T, Yao J, Duong T, Yang S, Zhu X (2017) A hybrid approach for power system security enhancement via optimal installation of flexible AC transmission system (FACTS) devices. Energies 10(9):1305. https://doi.org/10.3390/en10091305
9. Abido MA (2009) Power system stability enhancement using FACTS controllers: a review. Arab J Sci Eng 34(1B):153–172
10. Nabavi-Niaki A, Iravani MR (1996) Steady-state and dynamic models of unified power flow controller (UPFC) for power system studies. IEEE Trans Power Syst 11(4):1937–1943. https://doi.org/10.1109/59.544667
11. Gyugyi L, Sen KK, Schauder CD (1999) The interline power flow controller concept: a new approach to power flow management in transmission systems. IEEE Trans Power Deliv 14(3):1115–1123. https://doi.org/10.1109/61.772382
12. Ara AL, Kazemi A, NabaviNiaki SA (2011) Modelling of optimal unified power flow controller (OUPFC) for optimal steady-state performance of power systems. Energy Convers Manag 52(2):1325–1333. https://doi.org/10.1016/j.enconman.2010.09.030
13. Zang XP, Handschin E, Yao M (2001) Modeling of the generalized unified power flow controller (GUPFC) in a nonlinear interior point OPF. IEEE Trans Power Syst 16(3):367–373. https://doi.org/10.1109/59.93227010.1109/59.932270
14. Kumar A, Srivastava SC, Singh SN (2005) Congestion management in competitive power market: a bibliographical survey. Electr Power Syst Res 76(1):153–164. https://doi.org/10.1016/j.epsr.2005.05.001
15. Zhang W, Li F, Tolbert LM (2007) Optimal allocation of shunt dynamic VAR source SVC and STATCOM: a survey. In: IET conference publications, pp 507–507. https://doi.org/10.1049/cp:20062251
16. Kumar GVN, Kumar BS, Rao BV, Chowdary DD (2019) Enhancement of voltage stability using FACTS devices in electrical transmission system with optimal rescheduling of generators by brain storm optimization algorithm. In: Cheng S, Shi Y (eds) Brain storm optimization algorithms. Adaptation, learning, and optimization, vol 23. Springer, Cham. https://doi.org/10.1007/978-3-030-15070-9_11
17. Dash SP, Subhashini KR, Satapathy JK (2020) Optimal location and parametric settings of FACTS devices based on JAYA blended moth flame optimization for transmission loss minimization in power systems. Microsyst Technol 26:1543–1552. https://doi.org/10.1007/s00542-019-04692-w
18. Hasanvand S, Fallahzadeh-Abarghouei H, Mahboubi-Moghaddam E (2019) Power system security improvement using an OPA model and IPSO algorithm. SIMULATION 96(3):325–335. https://doi.org/10.1177/0037549719886356
19. Shafik MB et al (2019) Adaptive multi objective parallel seeker optimization algorithm for incorporating TCSC devices into

optimal power flow framework. IEEE Access. https://doi.org/10.1109/access.2019.2905266

20. Naderi E, Pourakbari-Kasmaei M, Abdi H (2019) An efficient particle swarm optimization algorithm to solve optimal power flow problem integrated with FACTS devices. Appl Soft Comput 80:243–262. https://doi.org/10.1016/j.asoc.2019.04.012

21. Sayed F, Kamel S, Yu J et al (2020) Optimal load shedding of power system including optimal TCSC allocation using moth swarm algorithm. Iran J Sci Technol Trans Electr Eng 44:741–765. https://doi.org/10.1007/s40998-019-00255-x

22. Gope S, Dawn S, Mitra R, Goswami AK, Tiwari PK (2019) Transmission congestion relief with integration of photovoltaic power using lion optimization algorithm. In: Bansal J, Das K, Nagar A, Deep K, Ojha A (eds) Soft computing for problem solving, Advances in intelligent systems and computing, vol 816. Springer, Singapore, pp 327–338. https://doi.org/10.1007/978-981-13-1592-3_25

23. Ahmad AAL, Sirjani R (2019) Optimal placement and sizing of multi-type FACTS devices in power systems using metaheuristic optimisation techniques: an updated review. Ain Shams Eng J. https://doi.org/10.1016/j.asej.2019.10.013

24. Bansal RC (2005) Optimization methods for electric power systems: an overview. Int J Emerg Electr Power Syst. Article 1021. https://doi.org/10.2202/1553-779x.1021

25. Fister I Jr, Fister D, Fister I (2013) A comprehensive review of cuckoo search: variants and hybrids. Int J Math Model Numer Optim 4(4):387–409. https://doi.org/10.1504/IJMMNO.2013.059205

26. Nguyen KP, Fujita G, Dieu VN (2015) Optimal placement and sizing of static VAR compensator using Cuckoo search algorithm. In: 2015 IEEE congress on evolutionary computation (CEC). https://doi.org/10.1109/cec.2015.7256901

27. Nguyen KP, Fujita G, Dieu VN (2016) Cuckoo search algorithm for optimal placement and sizing of static var compensator in large-scale power systems. JAISCR 6(2):59–68. https://doi.org/10.1515/jaiscr-2016-0006

28. Balasubbareddy M, Sivanagaraju S, Suresh CV (2015) Multi-objective optimization in the presence of practical constraints using non–dominated sorting hybrid cuckoo search algorithm. Eng Sci Technol Int J 18(4):603–615. https://doi.org/10.1016/j.jestch.2015.04.005

29. Dash P, Saikia LC, Sinha N (2015) Comparison of performances of several FACTS devices using Cuckoo search algorithm optimized 2DOF controllers in multi–area AGC. Electr Power Energy Syst 65:316–324. https://doi.org/10.1016/j.ijepes.2014.10.015

30. Abd Elazim SM, Ali ES (2016) Optimal power system stabilizers design via cuckoo search algorithm. Electr Power Energy Syst 75:99–107. https://doi.org/10.1016/j.ijepes.2015.08.018

31. Abd-Elazim SM, Ali ES (2016) Optimal location of STATCOM in multimachine power system for increasing loadability by Cuckoo Search algorithm. Electr Power Energy Syst 80:240–251. https://doi.org/10.1016/j.ijepes.2016.01.023

32. Kumar D, Gupta V, Jha RC (2016) Implementation of FACTS devices for improvement of voltage stability using evolutionary algorithm. In: 2016 IEEE 1st international conference on power electronics, intelligent control and energy systems (ICPEICES), pp 1–6. https://doi.org/10.1109/icpeices.2016.7853354

33. Rao B, Kumar GV, Sravana Kumar B, Naidu K (2017) Cuckoo search algorithm based optimal tuning of thyristor controlled series capacitor to enhance the line based voltage stability. Adv Sci Technol Lett 147:104–109. https://doi.org/10.14257/astl.2017.147.16

34. Venkateswara Rao B, Venkata Nagesh Kumar G (2017) Optimal parameter setting of UPFC and real power generation cost minimization using Cuckoo Search Algorithm. Int Electr Eng J 7(11):2440–2445

35. Sen D, Acharjee P (2017) Optimal placement of UPFC based on technoeconomic criteria by hybrid CSA–CRO algorithm. In: 2017 IEEE PES Asia-Pacific power and energy engineering conference (APPEEC), pp 1–6. https://doi.org/10.1109/appeec.2017.8308909

36. Gaur D, Mathew L (2018) Optimal placement of FACTS devices using optimization techniques: a review. IOP conference series: materials science and engineering 331(012023):1–16. https://doi.org/10.1088/1757-899X/331/1/012023

37. Moghavvemi M, Omar FM (1998) Technique for contingency monitoring and voltage collapse prediction. In: IEE proceedings—generation, transmission and distribution, vol 145, no 6, pp 634–640. https://doi.org/10.1049/ip-gtd:19982355

38. Mareli M, Twala B (2017) An adaptive Cuckoo search algorithm for optimization. Appl Comput Inf 14(2):107–115. https://doi.org/10.1016/j.aci.2017.09.001

39. Khokhar B, Parmar KS, Dahiya S (2012) An efficient particle swarm optimization with time varying acceleration coefficients to solve economic dispatch problem with valve point loading. Energy Power 2(4):74–80. https://doi.org/10.5923/j.ep.20120204.06

40. Adepoju GA, Komolafe OA (2011) Analysis and modelling of static synchronous compensator (STATCOM): a comparison of power injection and current injection models in power flow study. Int J Adv Sci Technol 36(2):65–76

41. Son KM, Lasseter RH (2004) A Newton–type current injection model of UPFC for studying low–frequency oscillations. IEEE Trans Power Deliv 19(2):694–701. https://doi.org/10.1109/TPWRD.2003.822543

42. Vural AM, Tumay M (2007) Mathematical modeling and analysis of a unified power flow controller: a comparison of two approaches in power flow studies and effects of UPFC location. Int J Electr Power Energy Syst 29(8):617–629. https://doi.org/10.1016/j.ijepes.2006.09.005

43. Lubis RS, Hadi SP, Tumiran (2011) Modeling of the generalized unified power flow controller for optimal power flow. In: Proceedings of international conference on electrical engineering and informatics (ICEEI), Bandung, Indonesia, pp 4577–0752, 17th–19th July, 2011. https://doi.org/10.1109/iceei.2011.6021763

44. Vyakaranam B, Villaseca FE (2014) Dynamic modeling and analysis of generalized unified power flow controller. J Electr Power Syst Res 106(5):1–11. https://doi.org/10.1016/j.epsr.2013.07.010

45. Yang XS (2014) Nature-inspired optimization algorithms, 1st edn. Elsevier, London, p 3. https://doi.org/10.1016/B978-0-12-416743-8.00017-8

46. Civicioglu P, Besdok E (2013) A conceptual comparison of the Cuckoo-search, particle swarm optimization, differential evolution and artificial bee colony algorithms. Artif Intell Rev 39(4):315–346. https://doi.org/10.1007/s10462-011-9276-0

47. Zheng H, Zhou Y (2012) A novel cuckoo search algorithm based on Gauss distribution. J Comput Inf Syst 8(10):4193–4200

48. Zaw MM, Mon EE (2014) Web document clustering using Gauss distribution based cuckoo search clustering algorithm. Int J Sci Eng Technol Res 3(13):2945–2949

49. Ho SD, Vo VS, Le TM, Nguyen TT (2014) Economic emission load dispatch with multiple fuel optings using cuckoo search algorithm with Gaussian and Cauchy distributions. Int J Energy Inf Commun 5(5):39–54. https://doi.org/10.14257/ijeic.2014.5.5.04

50. Nguyen TT, Vo DN, Dinh BH (2016) Cuckoo search algorithm using different distributions for short term hydrothermal scheduling with reservoir volume constraint. Int J Electr Eng Inf 8(1):76–92. https://doi.org/10.15676/ijeei.2016.8.1.6

51. Roy S, Mallick A, Chowdhury SS, Roy S (2015) A novel approach on cuckoo search algorithm using Gamma distribution. In: Second international conference on electronics and communication systems (ICECS), Coimbatore, pp 466–468. https://doi.org/10.1109/ecs.2015.7124948

52. Tusiy SI, Shawkat N, Ahmed MA, Panday B, Sakib N (2015) Comparative analysis on improved Cuckoo search algorithm and artificial bee colony algorithm on continuos optimization problems. Int J Adv Res Artif Intell 4(2):14–19. https://doi.org/10.14569/IJARAI.2015.040203

53. Tuba M, Subotic M, Stanarevic N (2011) Modified Cucko search algorithm for unconstrained optimization problems. In: Proceedings of the European computing conference

54. Zimmerman RD, Murillo-Sanchez CE, Thomas RJ (2011) MAT-POWER: steady–state operations, planning and analysis tools for power system research and education. IEEE Trans Power Syst 26(1):12–19

55. Achayuthakan, C, Ongsakul W (2009) TVAC–PSO based optimal reactive power dispatch for reactive power cost allocation under deregulated environment, In: IEEE conference on power & energy society general meeting, pp 26–30, July 2009. https://doi.org/10.1109/pes.2009.5275294

56. Wolpert DH, Macready WG (1997) No free lunch theorems for optimization. IEEE Trans Evolut Comput 1(1):67–82. https://doi.org/10.1109/4235.585893

P. V. R. L. Narasimham is born in 1964. He received B.Tech Degree from Andhra University in 1984. He received Master of Engineering degree from PSG College of Technology in 1987 and received Doctoral degree from Osmania University in 2012. He has 30 years of teaching experience. Currently he is working as Professor EEE in EEE Department, V R Siddhartha Engineering College, Vijayawada. His interested areas are Electric Drives, Power Electronics, Solar Power, FACTS.

K. V. Kumar Kavuturu is born in 1987. He received B.Tech and M.Tech Degrees from JNTU, Hyderabad in 2008 and 2011 respectively. He is currently pursuing Doctorial Degree from JNTU, Kakinada. His interested areas are FACTS, Voltage stability, Power Systems and Renewable Energy Sources.